

## Signature Inversion Caused by Triaxiality and Unpaired Band Crossings in $^{72}\text{Br}$

C. Plettner,<sup>1,2</sup> I. Ragnarsson,<sup>3</sup> H. Schnare,<sup>1</sup> R. Schwengner,<sup>1</sup> L. Käubler,<sup>1</sup> F. Dönau,<sup>1</sup> A. Algora,<sup>4</sup> G. de Angelis,<sup>4</sup> D. R. Napoli,<sup>4</sup> A. Gadea,<sup>5</sup> J. Eberth,<sup>6</sup> T. Steinhardt,<sup>6</sup> O. Thelen,<sup>6</sup> M. Hausmann,<sup>7</sup> A. Müller,<sup>7</sup> A. Jungclaus,<sup>7</sup> K. P. Lieb,<sup>7</sup> D. G. Jenkins,<sup>8</sup> R. Wadsworth,<sup>8</sup> and A. N. Wilson<sup>8</sup>

<sup>1</sup>*Institut für Kern- und Hadronenphysik, FZ Rossendorf, D-01314 Dresden, Germany*

<sup>2</sup>*Horia Hulubei National Institute of Physics and Nuclear Engineering, Bucharest, P.O. Box MG-6, Romania*

<sup>3</sup>*Department of Mathematical Physics, Lund Institute of Technology, P.O. Box 118, S-22100 Lund, Sweden*

<sup>4</sup>*INFN, Laboratori Nazionali di Legnaro I-35020, Legnaro, Italy*

<sup>5</sup>*Instituto de Fisica Corpuscular, ES-46071 Valencia, Spain*

<sup>6</sup>*Institut für Kernphysik, Universität zu Köln, D-50937 Köln, Germany*

<sup>7</sup>*II. Physikalisches Institut, Universität Göttingen, D-37073 Göttingen, Germany*

<sup>8</sup>*University of York, Physics Department, Heslington, York YO1 5DD, United Kingdom*

(Received 8 March 2000)

High-spin states in  $^{72}\text{Br}$  were studied with the EUROBALL III spectrometer using the  $^{40}\text{Ca}(^{40}\text{Ca}, \alpha 3p 1n)$  reaction. The negative-parity band observed in this experiment displays a signature inversion around spin  $I = 16$ . The interpretation within the cranked Nilsson-Strutinsky approach shows that this signature pattern is a signal of a substantial triaxial shape change with increasing spin where the nucleus evolves from a triaxial shape with rotation about the intermediate axis at low spin through a collective prolate shape to a triaxial shape but with rotation about the shortest principal axis at high spin.

PACS numbers: 21.10.Re, 23.20.En, 23.20.Lv, 27.50.+e

Rotational structures in nuclei can be characterized by the signature quantum number  $\alpha$  which defines the admissible spin sequence for a band through the relation  $I = \alpha + 2n$  ( $n = 0, 1, \dots$ ). This is a consequence of the well-known  $D_2$  symmetry of deformed intrinsic shapes reflected through the appearance of two signature partner bands with  $\alpha = 0$  or 1 in even-mass nuclei and  $\alpha = \pm \frac{1}{2}$  in odd-mass nuclei (note  $\alpha = \frac{3}{2} \equiv -\frac{1}{2}$ ). In a plot of the level energies  $E(I)$  vs  $I$  usually each of the two signature branches forms a regular  $I(I + 1)$  sequence. One branch is favored, i.e., lower in energy, whereas the other one is separated by the so-called signature splitting. Usually, one expects that such a signature splitting is growing with the spin  $I$  due to the increasing Coriolis force. Quantitatively this splitting effect can be seen when plotting the scaled energy differences  $[E(I) - E(I - 1)]/2I$  vs  $I$  which appear as a typical staggering curve. However, one observes in several cases that the signature splitting decreases with spin and even changes its sign, i.e., the energetically favored and unfavored signature branches cross each other and interchange their role. This phenomenon is known as signature inversion. It has been suggested that such an inversion might be a specific fingerprint for a triaxial shape in nuclei [1], but no conclusive evidence for this explanation has been presented so far. In an alternative interpretation, such a signature inversion may be caused by the residual interaction between high- $j$  particles [2].

The rotational bands considered previously with regard to signature inversion were based on high- $j$  orbitals. Our study of bands in  $^{72}\text{Br}$  represents a new situation, because here the low- $j$  orbitals of the  $fp$  shell play a crucial role and determine interesting properties. Since no large signature-dependent effects from residual interactions are

expected for these orbitals, only mean field contributions will be considered in the present study.

High-spin states in  $^{72}\text{Br}$  were populated in the reaction  $^{40}\text{Ca}(^{40}\text{Ca}, \alpha 3pn)$  at 185 MeV, using the  $^{40}\text{Ca}$  beam delivered by the XTU Tandem accelerator of the Laboratori Nazionali di Legnaro. We used a self-supporting  $^{40}\text{Ca}$  target with an enrichment of 99.96% and a thickness of 0.9 mg/cm<sup>2</sup>.  $\gamma$  rays were registered with the 15 Cluster [3] and 26 Clover [4] detectors of the EUROBALL III spectrometer. Charged particles were detected with the ISIS ball consisting of 40  $\Delta E - E$  silicon-detector telescopes [5]. At forward angles, 15 segmented detector units filled with BC501A liquid scintillator were mounted to detect neutrons [6]. Approximately  $2 \times 10^9$   $\gamma\gamma\gamma$  coincidences were collected and sorted off line into two-dimensional  $E_\gamma - E_\gamma$ -particle matrices and three-dimensional  $E_\gamma - E_\gamma - E_\gamma$  cubes. These coincidence data were analyzed using the Radware package [7].

The level scheme of the  $^{72}\text{Br}$  nucleus resulting from the present experiment is shown in Fig. 1. The relative spin values with respect to the ground state were deduced from an analysis of  $\gamma - \gamma$  directional correlations of oriented states. However, spins and parities remain tentative due to the tentative assignments for the ground state [8]. Based on the present spin and parity assignments, the excitation energies of states with given spin and parity in the chain of odd-odd Br isotopes [9–11] result in a smooth curve with respect to the neutron number. This comparison, previously applied to other mass regions [12], certainly fixes the spin within 1  $\hbar$ . The levels marked with thicker lines in Fig. 1 are the highest levels in the negative-parity bands known from previous studies [8,13]. In a very recent study the positive-parity bands were established up to

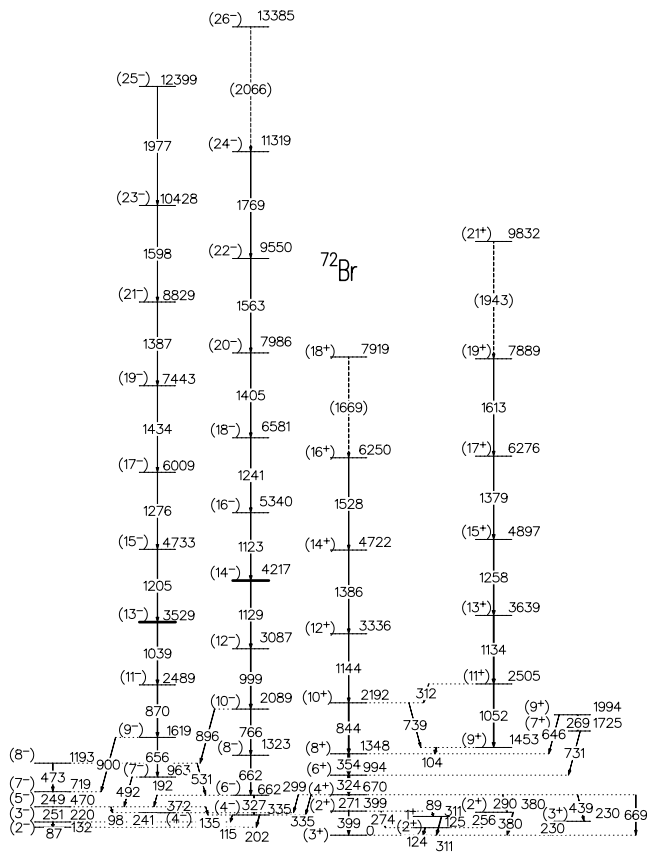


FIG. 1. The level scheme of  $^{72}\text{Br}$  obtained in the present experiment. For details of the low-spin part, see Ref. [13].

spin (21) [14], whereas negative-parity states were not reported. Based on the present coincidence measurement we extended the negative-parity bands to an excitation energy of  $E_x \approx 13$  MeV and a spin of  $I = (26)$ .

The negative-parity bands display peculiar features. Each of the two branches with signatures  $\alpha = 0$  and  $\alpha = 1$  shows a backbend, namely at  $I \approx 14$  and  $I \approx 19$ , respectively. However, the most surprising feature is the signature splitting that can be seen in Fig. 2(a). The  $\alpha = 1$  branch is favored up to  $I \approx 16$  where a crossing of the branches takes place such that the  $\alpha = 0$  branch is favored at higher spins. This signature inversion in the negative-parity bands is unique in the chain of odd-odd Br isotopes. In contrast, the  $^{74,76,78}\text{Br}$  nuclei display signature inversions in the positive-parity bands, at low spin values  $I \approx 9$  [9–11]. This phenomenon was theoretically predicted and discussed in Ref. [15]. The spin value where the inversion occurs corresponds to the maximum spin of a single-particle configuration with *one* proton and *one* neutron in the high- $j$   $g_{9/2}$  orbitals.

To understand the microscopic origin of the signature inversion in the negative-parity bands of  $^{72}\text{Br}$  we performed calculations using the configuration-dependent cranked Nilsson-Strutinsky (CNS) approach [16,17] to obtain the equilibrium shapes of selected configurations at different spin values. The parameters of the Nilsson

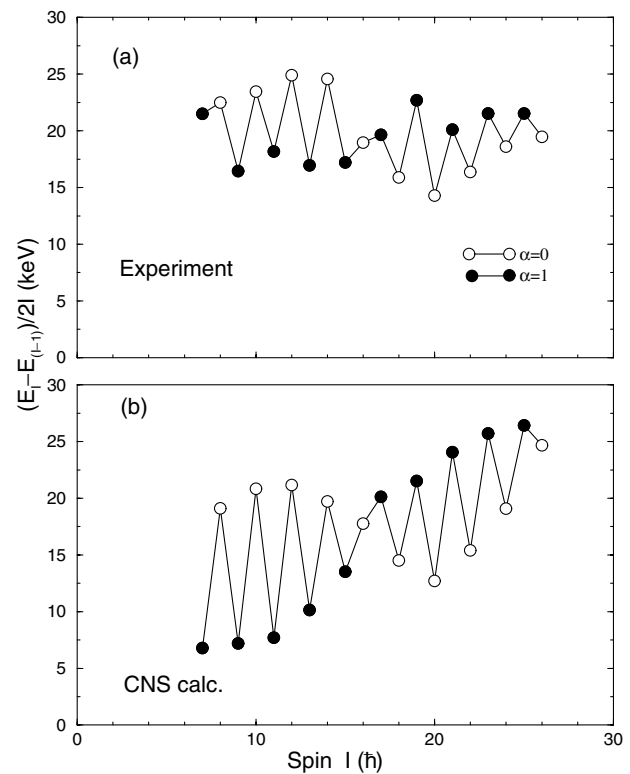


FIG. 2. The energy difference between the states with spin  $I$  and spin  $(I - 1)$ , divided by twice the spin, for the observed (a) and calculated (b) negative-parity band in  $^{72}\text{Br}$ .

potential adapted to  $A \approx 80$  nuclei [17] were used. The energies of the observed bands are plotted as a function of the spin in Fig. 3(a), with a standard rigid rotation reference subtracted [17]. The negative slope indicates that in all four bands, the angular momentum is built at a lower energy cost than for the reference rotation. In fact, the best fit of the energies in the negative parity bands by a  $(\hbar^2/2J)I(I + 1)$  rotor expression leads to a moment of inertia  $J$  being about 30% larger than the one implied in the standard reference. This large moment of inertia can be attributed to particularly large shell effects at normal deformation in this nucleus, where the low energy for  $I = 20$ –25 indicates a very favored configuration for these spin values. It also suggests that pairing correlations are of minor importance for all spin values. This is the justification why the calculations were performed without pairing.

In the CNS calculations equilibrium configurations at near-oblate or near-prolate shape compete at low and intermediate spin. Collective near-oblate configurations are generally lowest in energy up to spins  $I = 10$ –12. At higher spins, however, collective configurations at near-prolate equilibrium shapes are calculated to be lower in energy. The high-spin band of positive parity is well described by such a configuration [see Fig. 3(b)], which includes one proton and three neutrons excited to the  $g_{9/2}$  orbital, whereas the remaining six protons and six

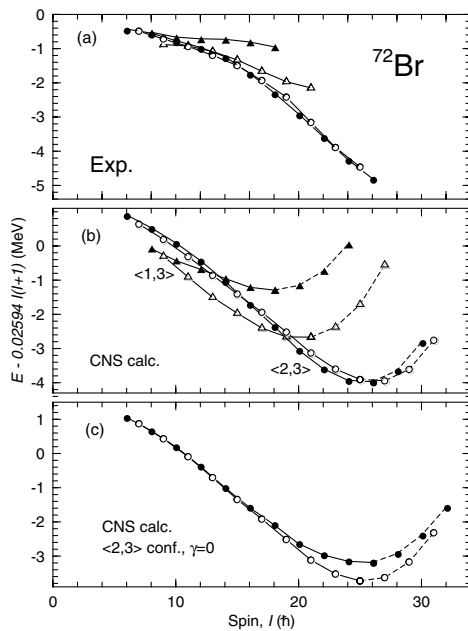


FIG. 3. Observed (a) and calculated (b,c) energies of high-spin bands in  $^{72}\text{Br}$  drawn vs spin  $I$  relative to a standard rigid rotation reference. The calculated energies have been normalized to the observed states around the signature crossing at  $I \approx 16$ . The calculated bands are labeled by the number of  $g_{9/2}$  protons and neutrons. In (b), a minimization in  $(\epsilon_2, \gamma, \epsilon_4)$  deformation was performed for each state, while in (c) the shape is constrained at  $\gamma = 0$  (axial symmetry).

neutrons above  $Z = 28$  stay in the  $N = 3$  orbitals. Accordingly, it is labeled  $\langle 1, 3 \rangle$  [17]. Indeed, the large signature splitting between the odd and even spin branches observed for the positive-parity band [14] can only be reproduced, if the unpaired nucleons are in high- $j$  intruder  $g_{9/2}$  orbitals, resulting in positive parity [Fig. 3(b)]. Moreover, the calculations predict the branch with signature  $\alpha = 1$  to be lower in energy, which is consistent with the experiment [Fig. 3(a) and 3(b)]. This is in agreement with general expectations for the signature splitting of a band based on high- $j$   $g_{9/2}$  orbitals [1,11], and implies that our spin values in these bands can be changed only in units of  $\Delta I = \pm 2$  (conserving the signature). Combined with the arguments given above this confirms the proposed spin values for the high-spin states in  $^{72}\text{Br}$ .

The CNS calculations show that the negative-parity band at high spin is well described by the near-prolate  $\langle 2, 3 \rangle$  configuration. This assignment is strongly supported by the small signature splitting observed experimentally for this band [Fig. 3(a)], which can be reproduced only with an unpaired nucleon in the low- $j$   $fp$  orbitals. The reliability of the present approach is further supported by the fact that a similar configuration describes the high-spin properties of the negative-parity bands in the neighboring  $^{73}\text{Br}$  nucleus [18].

We performed a fully consistent calculation, i.e., the equilibrium deformation in the potential energy surface

was searched for at each spin value separately. A comparison of the obtained signature splitting with the experimental one is shown in Fig. 2(b). It can be seen that the main features are reproduced in the calculations. The odd-spin branch ( $\alpha = 1$ ) is favored up to  $I \leq 16$ , whereas after the inversion the even-spin branch ( $\alpha = 0$ ) is lower in energy. Moreover, both branches approach again at the highest observed spin. This behavior is reflected in Fig. 3(b) and is consistent with the experimental findings given in Fig. 3(a).

In Fig. 3(c) a calculation with a fixed axial-symmetric shape ( $\gamma = 0^\circ$ ) and free deformation parameters  $\epsilon_2, \epsilon_4$  is presented. In this case, no signature splitting is predicted at low spin. Moreover, the prediction that the  $\alpha = 1$  branch is favored at  $I \approx 20$  is incorrect. At fixed negative  $\gamma$  values (triaxial shape with rotation about the intermediate principal axis) the signature order becomes correct at low spin, but no inversion occurs. On the other hand, at positive  $\gamma$  values (rotation about the short axis), the  $\alpha = 0$  branch is favored at low spin in contradiction to the experiment. This analysis shows clearly that the signature splitting and especially the signature inversion are reproduced only by a varying  $\gamma$  deformation with increasing spin as obtained from the fully consistent calculation. This changing  $\gamma$  deformation manifests itself in the calculated deformation trajectories, which connect the energy minima at different spins. These trajectories are graphed in Fig. 4(a). At low spin the equilibrium deformation corresponds to negative  $\gamma$  values ( $\gamma = -10^\circ$  to  $-15^\circ$ ). However, it gradually changes with increasing spin to positive values with  $\gamma = +15^\circ$  to  $+20^\circ$  at the highest observed spins. The maximum spins of the two signature branches of the configuration  $\langle 2, 3 \rangle$  are  $I_{\text{max}}^\pi = 30^-$  and  $31^-$ , respectively, if only the  $N = 3$  orbitals  $p_{3/2}$  and  $f_{5/2}$  are included. However, the calculations do not predict any distinct termination of the branches at these spins. Instead they continue to higher spins, which is mainly caused by coupling with the  $f_{7/2}$  orbital. These states of higher spin appear, however, at very high energies (cf. Ref. [17]).

A more detailed understanding of the microscopic features causing the behavior of the two signatures of the negative-parity band in  $^{72}\text{Br}$  is obtained from the Routhian diagram in Fig. 4(c) constructed for an average trajectory. This plot reveals the crossing of the two signature branches at  $I \approx 16$ . This crossing is caused by the interaction between the lowest  $f_{5/2}$  and the highest  $p_{3/2}$  orbitals. These have spin projections onto the symmetry axis of  $\Omega = 1/2$  and  $\Omega = 3/2$ , respectively, in the limit of axial symmetry. Thus, the odd particle is in the  $\Omega = 3/2$  orbital at low spin. Since only  $\Omega = 1/2$  orbitals have a first order signature splitting at axial symmetry (a decoupling factor  $a \neq 0$ ), this explains why no signature splitting is found at low spin in Fig. 3(c). A somewhat similar interaction between medium- $j$  orbitals leading to positive and negative  $\gamma$  deformation has been discussed for  $^{123}\text{La}$  in Ref. [19]. In that case, however, there is no support from the

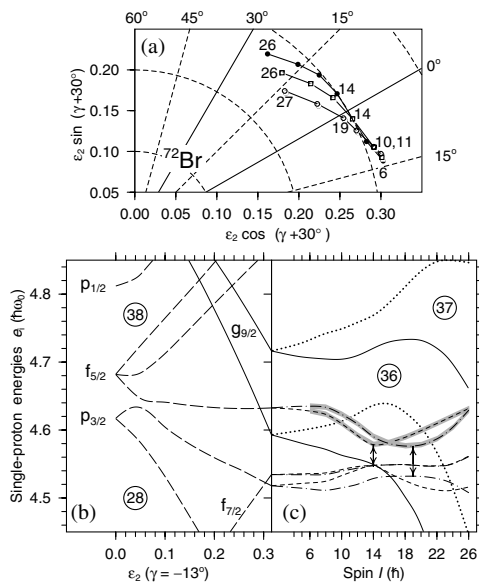


FIG. 4. (a) Calculated deformation trajectories for the even-spin (filled circles), odd-spin (open circles) states of the negative-parity bands in  $^{72}\text{Br}$  and an average trajectory (open squares) in steps of  $4\hbar$ . The origin of the orbitals at spherical shape is traced in (b). Routhians at deformations along the average trajectory at approximate spin values (c). The negative-parity configurations are formed relative to the  $Z = 36$  gap by making holes in orbitals shown on a shaded background. Arrows indicate the strongest interaction of these orbitals with the next lowest ( $f_{5/2}$ ,  $p_{3/2}$ ) orbitals. Since neutron and proton orbitals are similar, the graph indicates a low level density (favored shell energy) at high spin for  $Z, N = 35-37$ .

experiment, because no specific fingerprint pointing to triaxial deformation was identified, and only one signature was experimentally observed.

It is finally interesting to note the spin values where the orbitals interact in Fig. 4(c). For signature  $\alpha = 1/2$ , this occurs at  $I \approx 14$  in agreement with the band crossing observed in the even-spin branch. Analogously, the interaction occurs at  $I \approx 19$  for the  $\alpha = -1/2$  orbitals, which is consistent with the observed band crossing in the odd-spin branch. Thus, the observed band crossings can be understood as crossings (local interactions) between unpaired orbitals. This is compatible with our assumption that pairing correlations are negligible in these bands.

In summary, the signatures  $\alpha = 0$  and  $\alpha = 1$  of the negative-parity bands in  $^{72}\text{Br}$  were observed up to  $I = (26)$  and  $I = (25)$ , respectively. The moments of inertia of these bands exceed the rigid-body value indicating large effects from the specific shell structure of this nucleus. A detailed description of these bands is achieved in terms of cranked Nilsson-Strutinsky calculations with standard parameters. The two signature branches cross

around  $I \approx 16$ . The occurrence of a signature inversion in this spin region is reproduced in the calculations, if the self-consistent deformation is determined for each state separately. The calculated sequences start at a triaxial deformation with rotation about the intermediate axis ( $\gamma = -10^\circ$  to  $-15^\circ$ ) but change their deformation as a function of the spin and become triaxial with rotation about the shortest principal axis ( $\gamma = +15^\circ$  to  $+20^\circ$ ) at the highest spins. A study of the microscopic background shows that the signature inversion cannot be obtained without this specific shape evolution. Furthermore, a band crossing observed at different spins in the two signature branches is explained as being due to unpaired crossings (local interactions) between the two signature branches of the lowest  $f_{5/2}$  orbital and the highest  $p_{3/2}$  orbital.

This work was supported by the German Ministry of Education and Research under Contracts No. 06 DR 827, No. 06 OK 862, and No. 06 GOE 851, by the Swedish Natural Science Research Council, by the UK EPSRC, and by the European Union within the TMR Project No. ERBFMGECT 980110.

- [1] R. Bengtsson *et al.*, Nucl. Phys. **A415**, 189 (1984).
- [2] R. A. Bark *et al.*, Nucl. Phys. **A630**, 603 (1998), and references therein.
- [3] J. Eberth, Nucl. Instrum. Methods Phys. Res., Sect. A **369**, 135 (1996).
- [4] F. A. Beck *et al.*, in *Proceedings of the Conference on Physics from Large  $\gamma$ -ray Detector Arrays, Berkeley, 1994* (LBL 35687, CONF 940888, UC 413), p. 154.
- [5] E. Farnea *et al.*, Nucl. Instrum. Methods Phys. Res., Sect. A **400**, 87 (1997).
- [6] Ö. Skeppstedt *et al.*, Nucl. Instrum. Methods Phys. Res., Sect. A **421**, 531 (1999).
- [7] D. C. Radford, Nucl. Instrum. Methods Phys. Res., Sect. A **361**, 297 (1995).
- [8] G. Garcia Bermudez *et al.*, Phys. Rev. C **25**, 1396 (1982).
- [9] J. Döring *et al.*, Phys. Rev. C **47**, 2560 (1993).
- [10] Q. Pan *et al.*, Nucl. Phys. **A627**, 334 (1997).
- [11] E. Landulfo *et al.*, Phys. Rev. C **54**, 626 (1996).
- [12] Yunzuo Liu, Jingbin Lu, Yingjun Ma, Shangui Zhou, and Hua Zheng, Phys. Rev. C **54**, 719 (1996).
- [13] S. Ulbig *et al.*, Z. Phys. A **329**, 51 (1988).
- [14] N. Fotiadis *et al.*, Phys. Rev. C **60**, 057302-1 (1999).
- [15] A. J. Kreiner and M. A. J. Mariscotti, Phys. Rev. Lett. **43**, 1150 (1979).
- [16] T. Bengtsson and I. Ragnarsson, Nucl. Phys. **A436**, 14 (1985).
- [17] A. V. Afanasjev *et al.*, Phys. Rep. **322**, 1 (1999).
- [18] C. Plettner *et al.*, Phys. Rev. C **62**, 014313 (2000).
- [19] R. Wyss *et al.*, Nucl. Phys. **A503**, 244 (1989).